

# Non-invasive steel haunch upgradation strategy for seismically deficient reinforced concrete exterior beam-column sub-assemblages

A. Kanchanadevi <sup>\*1,2</sup> and K. Ramanjaneyulu <sup>1,2a</sup>

<sup>1</sup> CSIR-Structural Engineering Research Centre, Chennai, 600113, Tamil Nadu, India

<sup>2</sup> Academy of Scientific and Innovative Research (AcSIR), Chennai, 600113, Tamil Nadu, India

(Received October 14, 2017, Revised June 7, 2018, Accepted July 16, 2018)

**Abstract.** Prior to the introduction of modern seismic guidelines, it was a common practice to provide straight bar anchorage for beam bottom reinforcement of gravity load designed building. Exterior joints with straight bar anchorages for beam bottom reinforcements are susceptible to sudden anchorage failure under load reversals and hence require systematic seismic upgradation. Hence in the present study, an attempt is made to upgrade exterior beam-column sub-assembly of a three storied gravity load designed (GLD) building with single steel haunch. Analytical formulations are presented for evaluating the haunch forces in single steel haunch retrofit. Influence of parameters that affect the efficacy and effectiveness of the single haunch retrofit are also discussed. The effectiveness of the single haunch retrofit for enhancing seismic performance of GLD beam-column specimen is evaluated through experimental investigation under reverse cyclic loading. The single steel haunch retrofit had succeeded in preventing the anchorage failure of beam bottom bars of GLD specimen, delaying the joint shear damage and partially directing the damage towards the beam. A remarkable improvement in the load carrying capacity of the upgraded GLD beam-column sub-assembly is observed. Further, a tremendous improvement in the energy dissipation of about 2.63 times that of GLD specimen is observed in the case of upgraded GLD specimen. The study also underlines the efficacy of single steel haunch retrofit for seismic upgradation of deficient GLD structures.

**Keywords:** gravity load designed; beam-column sub-assembly; upgradation; steel haunch; energy dissipation; strength and stiffness degradation

## 1. Introduction

Majority of reinforced concrete framed buildings built prior to 1970s are gravity load designed (GLD) structures. In general, existence of deeper beam section than the column section with inadequate longitudinal column reinforcements is the most common feature of the GLD buildings built all over the world. This resulted in the weak-column and strong beam scenario and in turn lead to the soft storey mechanism (Aycardi *et al.* 1994, Bracci *et al.* 1995). Absence/insufficiency of transverse reinforcement in the joint region of GLD frames results in the beam-column joint failure under seismic loading; leading to huge strength degradation locally and thereby reducing the lateral load carrying capacity of the structure globally and often associated with increased storey drifts (Paulay and Priestley 1992, Tsonos 1999, Pampanin *et al.* 2006). Insufficient anchorage of the beam bottom reinforcement of GLD frames leads to the anchorage failure or brittle bond failure under seismic loading, which in turn results in huge strength degradation (Kanchanadevi and Ramanjaneyulu 2017). On the whole, GLD framed buildings lack confinement, possess insufficient transverse- and main- reinforcement in

beam and column, and had insufficient connection detailing to cater for seismic forces. All these inherent weaknesses resulted in poor seismic performance of GLD framed buildings, as witnessed during the past earthquakes such as Northridge (1994) and Bhuj (2001) earthquakes of magnitude 6.7 and 7.7 respectively (Goltz 1994, Bokey and Pajgade 2004). GLD structures are existing even in the zones of higher and moderate seismicity. In order to prevent catastrophic failure and to improve the seismic performance of GLD structures, it is highly essential to devise seismic upgradation strategies for the existing GLD structures. Further, it may be noted that the exterior beam-column sub-assemblages in a GLD framed building are more vulnerable as they do not possess proper force transfer mechanism and are prone to anchorage failures. Hence, development of feasible upgradation scheme for the exterior beam-column joints of existing GLD building and evaluation of their seismic performance in terms of the seismic performance parameters is the active area of research.

Several researchers made attempts to retrofit/upgrade the deficient beam-column sub-assemblages using composite construction techniques such as near surface mounting, jacketing, Fiber reinforced polymer (FRP) strengthening, steel haunch retrofitting, joint enlargement, strengthening with steel elements etc. Recent works on jacketing of seismically deficient reinforced concrete members, focused on the usage of high performance concrete / hybrid methods i.e., combination of methods.

\*Corresponding author, Ph.D. Student,  
E-mail: [kanchana@serc.res.in](mailto:kanchana@serc.res.in)

<sup>a</sup> Ph.D.

Shannag *et al.* (2002) used high performance fiber reinforced concrete (HPFRC) jacket around the joint region and was successful in preventing the brittle joint shear failure. Further, the ductile failure was observed in the repaired specimens. Similarly, Dogan and Opara (2003) used slurry-infiltrated fiber concrete and slurry-infiltrated mat concrete jackets for retrofitting of interior beam-column joints and succeeded in preventing the brittle modes of failure. Adam *et al.* (2008) used the combination of steel angles and strips along with mortar for the strengthening of axial load dominating interior columns of framed buildings and improved the ultimate load capacity. Hadi and Tran (2014) used concrete covers together with CFRP jacketing for strengthening and repairing the seismically deficient reinforced concrete exterior beam-column joints and improved the seismic performance of both repaired and strengthened specimens. Tsonos (2014) used steel fiber concrete of high and ultra-high strength for jackets without additional reinforcement for retrofit of old reinforced concrete structures. This method was found to be much more effective than the conventional reinforced concrete jackets. Kalogeropoulos *et al.* (2016) used combination of extension bars, steel plates and RC jacketing of columns to retrofit the exterior beam column sub-assemblages and the retrofitted specimen showcased superior seismic performance compared with deficient specimen. The specimen retrofitted only by RC jacketing showed poor seismic performance similar to that of the control specimen. Bansal *et al.* (2016) used ferro-cement jackets for retrofitting of deficient exterior beam-column sub-assemblages. The retrofitted specimens showed improvement in load carrying capacity but there was no improvement in ductility and energy dissipation. Even though jacketing is the most effective method of retrofitting, it is highly laborious, expensive, difficult to implement and hinder the occupancy of the buildings.

The FRP strengthening of beam-column sub-assemblages possess lot of advantages, such as easy to handle, easy installation and does not increase the member size, when compared with the conventional jacketing techniques. In this type, strengthening of the beam-column sub-assemblages was accomplished by providing FRP laminates or FRP sheets around the beam-column sub-assemblages or by combination of FRP, NSM and steel reinforcements (Gergely *et al.* 2000, El-Amoury and Ghobarah 2002, Ghobarah and Said 2002, Prota *et al.* 2004, Pampanin *et al.* 2007, Sezen 2012, Akguzel and Pampanin 2012, Realfonzo *et al.* 2014, Hadigheh *et al.* 2014, Fakharifar *et al.* 2014, Yurdakul and Avşar 2015). The difficulties with the FRP strengthening are: need for providing proper anchorage and poor performance under fire.

Further, strengthening of sub-assemblages were also done by providing steel cages, steel props and curbs, prestressed steel angles or steel L profiles on top and bottom faces of the floor beam (Sharbatdar *et al.* 2012, Shafaei *et al.* 2014, Campione *et al.* 2015, Santarsiero, 2015, Kheyroddin *et al.* 2016, Adibi *et al.* 2017). In addition to the above, retrofitting of exterior beam-column sub-assemblages were also carried out by providing the alternate force flow path by providing steel haunch between

beam and column. The concept of haunch retrofit solution was perceived by Yu *et al.* (2000) for steel moment resisting frames in view of significant failure of welds during Northridge earthquake. The concept of this haunch strengthening scheme was adopted and implemented for GLD RC structures by Pampanin and Christopoulos (2003) and Pampanin *et al.* (2006) by providing double haunches, one each at top and bottom faces of the floor beam. Joint damage was avoided and a flexural plastic hinge was formed in the beam at the point of haunch-beam connection. Genesio (2012) and Sharma *et al.* (2014) investigated the performance of double haunch system connected to the beam and column through post-installed anchors. The major drawbacks of strengthening measures detailed above are: (i) requires complete access of both beam and column segments for the proper implementation of the scheme; and (ii) causes hindrance to the occupancy of floor area.

From the reported studies, it could be noted that many attempts were made to improve the performance of the seismically deficient beam-column sub-assemblages through different retrofit measures and is the active area of research as on date. Further, it could be observed that most of these retrofit schemes are laborious, expensive, difficult to implement and hinder the occupancy of the buildings. Hence, in the present study, the emphasis is on the formulation of non-invasive, easily implementable scheme for upgradation of seismically deficient beam-column sub-assemblages. Therefore, in the present study, an exterior beam-column sub-assemblage is upgraded with single haunch upgradation strategy (SHUS) as it involves access only to the bottom of floor beam and side face of adjoining column. Analytical formulations are presented for evaluating the haunch forces for the most practical case of haunch connection with the adjoining members for aiding the design of single haunch retrofit. Further, the influence of different parameters viz., angle of inclination of steel haunch, effective moment of inertia of the reinforced concrete beam and column members, and stiffness of the haunch on the effectiveness of the SHUS is also presented. In order to evaluate the efficacy and effectiveness of SHUS, experimental investigations are carried out on an exterior beam-column sub-assemblage of typical three storied GLD building. The efficacy and effectiveness of SHUS in enhancing the seismic performance of GLD beam column sub-assemblage, in terms of load carrying capacity, energy dissipation, strength and stiffness degradation, is demonstrated by comparing the responses of upgraded GLD specimen with that of control GLD specimen. SHUS is primarily aimed to avoid the anchorage failure of beam bottom reinforcement of GLD beam-column sub-assemblage, delaying the joint failure mechanism as far as possible and redirecting partially the failure towards the beam.

## 2. Mechanism of Single steel haunch upgradation strategy (SHUS) and design consideration

In a typical single steel haunch upgradation scheme, steel bracing is introduced by connecting the adjoining beam and column segments. For providing quick insight

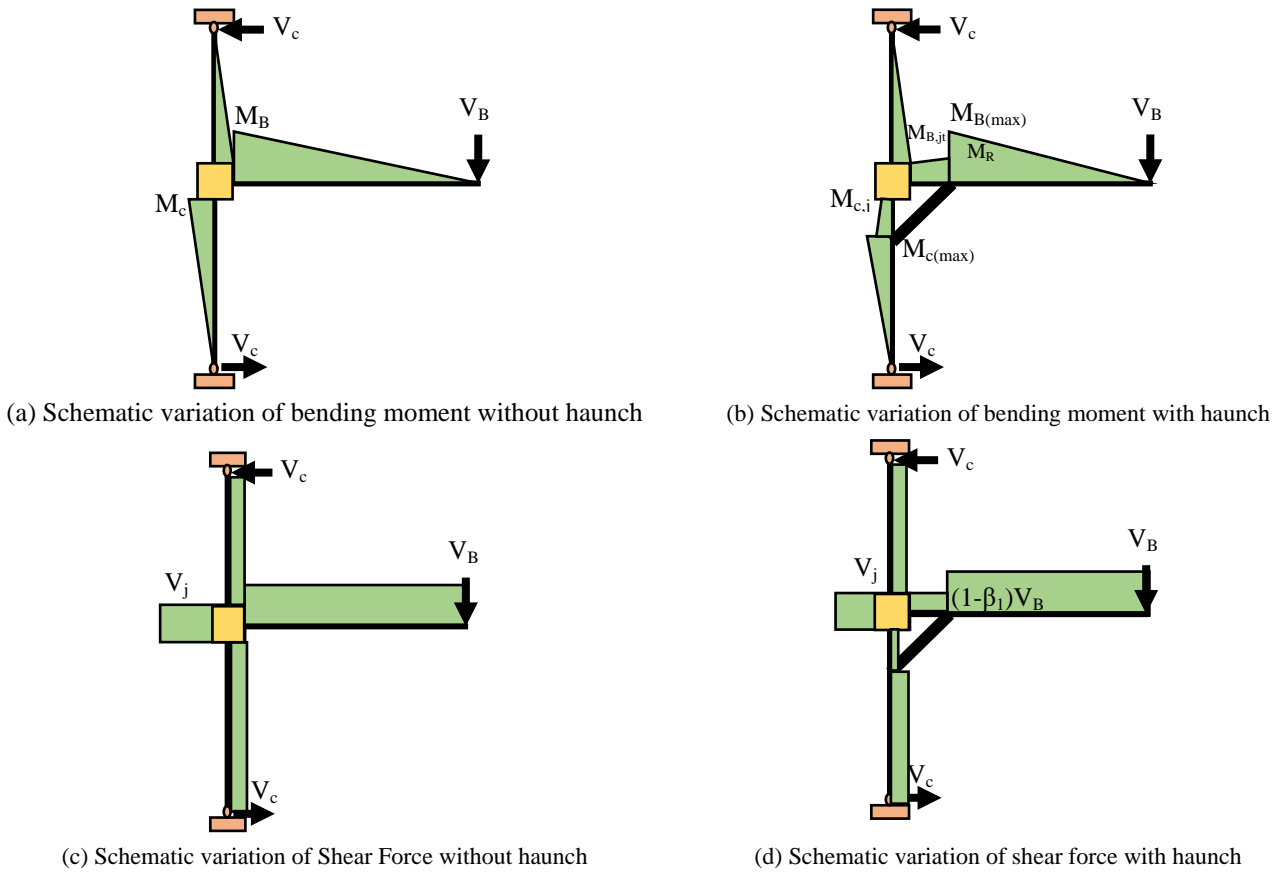


Fig. 1 Distribution of forces in beam-column sub-assembly with and without haunch under lateral load

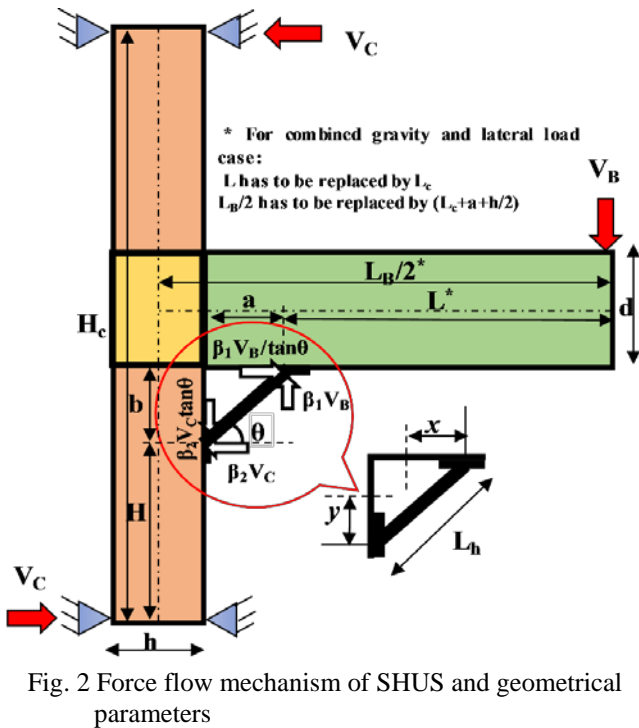


Fig. 2 Force flow mechanism of SHUS and geometrical parameters

flow in beam-column sub-assembly with SHUS and geometrical parameters of SHUS are shown in Fig. 2. The introduction of haunch produces vertical and horizontal forces at the haunch-beam and haunch-column connections (Fig. 2). The vertical component of haunch force is expressed as fraction ( $\beta_1$ ) of beam shear, where  $\beta_1$  is the ratio of vertical component of haunch force to beam shear. The vertical component of the haunch force introduces the shear opposite to beam shear and horizontal component of the haunch force at beam bottom produces a constant moment about the beam center in opposite direction to that due to loading at the beam tip. Thus, there would be reduction in the beam and column bending moments due to vertical and horizontal components of haunch forces (see Fig. 1(b)). Similarly, the reduction in column and beam shear due to haunch forces is shown in Fig 1(d). The efficacy of the haunch retrofit scheme is governed by  $\beta_1$ , which in turn depends on the stiffness and orientation of the haunch with the horizontal. The relation between  $\beta_1$  and  $\beta_2$  can be obtained by considering the equilibrium of forces.

Once the haunch forces are known, the reduced beam moment at the face of joint could be established as given below

$$M_{B,jt} = M_{B(max)} - M_R + (1 - \beta_1)V_B \cdot a \tag{1}$$

$$M_R = \frac{\beta_1 V_B d}{2 \tan \theta} \tag{2}$$

Where  $d$  = depth of beam;  $M_{B(max)} = V_B L$

into the beneficial effects of single haunch retrofit, schematic variations of the bending moment and shear force in beam-column sub-assembly with and without single haunch, due to lateral load, are shown in Fig. 1. The force

The moment at joint face can be obtained as

$$M_{B,jt} = M_{B(\max)} \left[ 1 - \frac{\beta_1 d}{2L \tan \theta} + \frac{(1 - \beta_1)a}{L} \right] \quad (3)$$

Similarly, reduced column moment at the face of the joint ( $M_{C,jt}$ ) is given as

$$M_{C,jt} = M_{C(\max)} \left[ 1 - \frac{\beta_2 h \tan \theta}{2H} + \frac{(1 - \beta_2)a \tan \theta}{H} \right] \quad (4)$$

Where,  $M_{C(\max)} = V_c H$ ;  $L = (L_B - h)/2 - a$ ;  $h$ —depth of column and  $d$ —depth of beam,  $M_{B,jt}$  is beam moment at the face of the joint,  $M_{B(\max)}$  is maximum moment in the beam at haunch location,  $M_R$  is reduction in beam moment due to horizontal component of the haunch force and the other notations used are presented pictorially in Figs. 1 and 2.

The effectiveness of the haunch upgradation depends on the magnitude of  $\beta_1$ . The value of  $\beta_1 = 1$  produces a shear exactly equal to the shear due to lateral load and thus, the beam moment at joint face would be equal to the maximum moment minus reduced moment ( $M_R$ ) and shear force in beam would be zero at the face of the joint. When  $\beta_1 = 2$ , the shear produced by the vertical component of haunch force would be exactly equal and opposite to the beam shear. Thus, there will be linear reduction in the beam moment towards the joint region. The value of  $\beta_1 > 2$  will introduce a higher shear demand in the beam than the actual shear due to lateral loads and hence the most important aspect of single haunch upgradation scheme (SHUS) is to choose value of  $\beta_1$  most appropriately. Similar arguments hold good for  $\beta_2$  and reduction in column moment and column shear depend on value of  $\beta_2$  which in turn depends on the orientation angle of haunch and  $\beta_1$ . Thus, the evaluation of  $\beta_1$  is the most significant aspect for the design of SHUS.

Yu *et al.* (2000) presented formulations for evaluation of haunch force for retrofitting of steel moment resisting frames with single steel haunch by considering the local deformation compatibility between the haunch and beam. The expression was developed for  $\beta_1$  by assuming the column to be rigid i.e., by accounting the flexural deformation of beam alone. For reinforced concrete structures, the magnitude of column deformation will be very large and hence the influence of column deformation has to be accounted (Pampanin *et al.* 2006). It was reported that the value of  $\beta_1$  estimated by incorporating the flexibility of the beam, column and shear deformation of the joint was very close to the value predicted by incorporating the flexibility of beam and column and without considering shear deformation of joint (Pampanin *et al.* 2006). Further, Pampanin *et al.* (2006) developed the formulation for the case of double haunch system, one each connected at the top and bottom faces of the floor beam by assuming point of contraflexure at the centre of the beam i.e., for the case of lateral load alone acting on the building frame. The expressions for the value of  $\beta_1$  with single haunch for the reinforced concrete structures are not reported in the

literature. Hence, in the present study expressions for the evaluation of  $\beta_1$  are derived for reinforced concrete exterior beam-column sub-assembly retrofitted with single steel haunch at the bottom of the floor beam by considering flexibility of beam as well as column. At first formulations are presented to evaluate the magnitude of  $\beta_1$  for lateral load alone case. In the case of gravity load dominated structures, i.e., when the moderate seismic risk is expected, lateral load would be smaller compared with gravity load and point of contraflexure would not be at the centre of beam. Hence, formulations for evaluating haunch forces of SHUS are extended for the case of combined gravity and lateral load case for two different types of connections of haunch, namely: (i) integral connection; and (ii) post-installed anchor connection system with the structural elements.

### 2.1 Evaluation of haunch force factor $\beta_1$ for the case of lateral loads alone acting

From the equilibrium of forces and considering the deformation compatibility at steel haunch-beam connection, the value of  $\beta_1$  is obtained as follows:

The beam moment at a distance 'x' from the haunch-beam connection (vide Fig. 2) is given by

$$M_x = \left( L - \frac{\beta_1 d}{2 \tan \theta} \right) V_B + (1 - \beta_1) V_B x \quad (5)$$

The stress induced in the beam at section 'x' from the beam-haunch connection, due to the moment and axial force is given by

$$\sigma_x = \frac{LV_B d}{2I_B} + \frac{V_B x d}{2I_B} - \frac{\beta_1 V_B x d}{2I_B} - \frac{\beta_1 V_B d^2}{4I_B \tan \theta} - \frac{\beta_1 V_B}{\tan \theta A_B} \quad (6)$$

The horizontal ( $\Delta_{bh}$ ) and vertical ( $\Delta_{bv}$ ) deformations of beam at the haunch location are given by

$$\Delta_{bh} = \int_0^a \frac{\sigma_x dx}{E_c} \quad (7)$$

$$\Delta_{bv} = \int_0^a \frac{M_x x dx}{E_c I_B} \quad (8)$$

After integration, the deformations are given by

$$\Delta_{bh} = \frac{V_B}{E_c I_B} \left[ \frac{Lad}{2} + \frac{a^2 d}{4} - \frac{\beta_1 a^2 d}{4} - \frac{\beta_1 a d^2}{4 \tan \theta} - \frac{\beta_1 a I_B}{A_B \tan \theta} \right] \quad (9)$$

$$\Delta_{bv} = \frac{V_B}{E_c I_B} \left[ \frac{La^2}{2} + \frac{a^3}{3} - \frac{\beta_1 a^2 d}{4 \tan \theta} - \frac{\beta_1 a^3}{3} \right] \quad (10)$$

Similarly, column moment at a distance 'y' from the haunch-column connection is given by

$$M_y = (H + y)V_C - \beta_2 V_C y - \frac{\beta_2 V_C h \tan \theta}{2} \quad (11)$$

The stresses developed at the section 'y' from the column-haunch connection is given by

$$\sigma_y = \frac{(H+y)V_c h}{2I_c} - \frac{\beta_2 V_c y h}{2I_c} - \frac{\beta_2 V_c \tan \theta h^2}{4I_c} - \frac{\beta_2 V_c \tan \theta}{A_c} \quad (12)$$

The horizontal ( $\Delta_{ch}$ ) and vertical ( $\Delta_{cv}$ ) deformations of the column at the location of haunch are given by

$$\Delta_{ch} = \int_0^b \frac{\sigma_y dy}{E_c} \quad (13)$$

$$\Delta_{cv} = \int_0^b \frac{M_y y dy}{E_c I_c} \quad (14)$$

After integration, the horizontal and vertical deformations are given by

$$\Delta_{ch} = -\frac{V_c}{E_c I_c} \left[ \frac{Hhb}{2} + \frac{b^2 h}{4} - \frac{\beta_2 \tan \theta h^2 b}{4} - \frac{\beta_2 b \tan \theta I_c}{A_c} - \frac{\beta_1 b^2 h}{4} \right] \quad (15)$$

$$\Delta_{cv} = -\frac{V_c}{E_c I_c} \left[ \frac{Hb^2}{2} + \frac{b^3}{3} - \frac{\beta_2 b^3}{3} - \frac{\beta_2 h \tan \theta b^2}{4} \right] \quad (16)$$

$$\text{Where, } \beta_2 = \frac{2\beta_1 H_c}{L_B \tan \theta} \quad (17)$$

where,  $A_c$  = area of cross section of column;  $A_b$  = area of cross section of beam;  $E_c$  = Young's Modulus of concrete;  $I_B$  = effective moment of inertia of beam;  $I_c$  = effective moment of inertia of Column;

From the deformation compatibility between beam-column sub-assemblages and haunches we have

$$\begin{aligned} & (\Delta_{bh} \cos \theta + \Delta_{bv} \sin \theta) - (\Delta_{ch} \sin \theta + \Delta_{cv} \cos \theta) \\ &= \frac{\beta_1 V_B L_h}{\sin \theta A_h E_s} \end{aligned} \quad (18)$$

After simplification, the value of  $\beta_1$  is obtained as given below

$$\beta_1 = \frac{b}{a} \left( \frac{N_1 + N_2}{D_1 + D_2} \right) \quad (19)$$

Where

$$\begin{aligned} N_1 &= 6Ld + 3ad + 6Lb + 4ab \\ N_2 &= \frac{3Hb^2 L_B I_B}{aH_c I_c} + \frac{2b^3 L_B I_B}{aH_c I_c} + \frac{3Hhb^2 L_B I_B}{a^2 H_c I_c} + \frac{3hb^3 L_B I_B}{2a^2 H_c I_c} \\ D_1 &= 6bd + 3d^2 + 4b^2 + \frac{12I_B}{A_B} + \frac{12I_B E_c}{aK_h \cos^2 \theta} \\ D_2 &= \frac{3h^2 b^3 I_B}{I_c a^3} + \frac{12b^3 I_B}{A_c a^3} + \frac{6b^3 h I_B}{I_c a^2} + \frac{4b^3 I_B}{I_c a} \end{aligned}$$

$K_h = A_h E_s / L_h$  is the stiffness of the haunch;  $A_h$  = area of cross section of haunch;  $E_s$  = Young's Modulus of steel;  $L_h$  = Length of haunch.

## 2.2 Evaluation of haunch force factor $\beta_1$ for the case of combined gravity and lateral loads

### 2.2.1 For integral connection

The value of  $\beta_1$  determined in the preceding section is based on the assumption that the point of contra-flexure of the beam is located at the centre of the beam, which holds good for lateral load dominating frames. For gravity load dominating frames, the value of  $\beta_1$  is determined by considering the actual point of contra-flexure (Fig. 2). Hence, the equations for  $\beta_1$  and  $\beta_2$  are modified accordingly to account for the actual point of contra-flexure as given below, by replacing 'L' with ' $L_c$ ' and representing  $L_B$  in terms of  $L_c$

$$\text{Where, } \beta_2 = \frac{2\beta_1 H_c}{(2L_c + 2a + h) \tan \theta} \quad (20)$$

Where  $L_c$  is length of beam between point of contra flexure and haunch-beam connection.

$$\beta_1 = \frac{b}{a} \left( \frac{E_1 + E_2 + E_3}{D_1 + D_2} \right) \quad (21)$$

Where

$$\begin{aligned} E_1 &= 6L_c d + 3ad + 6L_c b + 4ab \\ E_2 &= \frac{3Hb^2 (2L_c + 2a + h) I_B}{aH_c I_c} + \frac{2b^3 (2L_c + 2a + h) I_B}{aH_c I_c} \\ E_3 &= \frac{3Hhb^2 (2L_c + 2a + h) I_B}{a^2 H_c I_c} + \frac{3hb^3 (2L_c + 2a + h) I_B}{2a^2 H_c I_c} \end{aligned}$$

### 2.2.2 For Post-installed connection system

The Eqs. (20) and (21) for the evaluation of  $\beta_1$  and  $\beta_2$  are valid only when the haunch is integrally connected with beam and column i.e., using pretension anchor systems as used by Pampanin *et al.* (2006). For connection of haunch with adjacent beam and column by post-installed anchors, stiffness of haunch ( $K_h$ ) should be replaced by effective stiffness ( $K_E$ ) of haunch and post-installed anchor system in the Eq. (21) for the combined gravity and lateral load case.

The effective stiffness of the haunch and anchor system has to be evaluated by considering haunch and anchor as two springs in series. Thus, for evaluating the effective stiffness of haunch and anchor system, Genesio (2012), presented expressions for two limiting conditions, namely: (i) the concrete members under the haunches are considered to be rigid; (ii) the concrete members under the haunches are considered to be deformable. The actual behavior of the system would be in between these two cases.

The effective tensile stiffness of the haunch with rigid concrete member beneath it is given by

$$K_E = 1 / \left( \frac{\sin \theta}{K_N} + \frac{\cos \theta}{K_N} + \frac{1}{K_h} \right) \quad (22)$$

When  $\theta = 45$  degree,  $\sin \theta = \cos \theta$  and the Eq. (22) reduces to

$$K_E = 1 / \left( \frac{2\sin \theta}{K_N} + \frac{1}{K_h} \right) \quad (23)$$

Where,  $K_h$  = Stiffness of the haunch

$K_N$  = the tensile stiffness of the anchorage =  $nk_N$   
(number of anchors in the group  $x$  tensile stiffness of the single anchor)

$K_V$  = shear stiffness of the anchorage evaluated =  $nk_V$   
(number of anchors in the group  $x$  shear stiffness of the single anchor)

The effective tensile stiffness of the haunch with deformable concrete member beneath it is given by

$$K_E = 1 / \left( \frac{1}{\sqrt{(nK_N \sin \theta)^2 + (nK_V \cos \theta)^2}} + \frac{1}{\sqrt{(nK_N \cos \theta)^2 + (nK_V \sin \theta)^2}} + \frac{1}{K_h} \right) \quad (24)$$

When  $\theta = 45$  degree,  $\sin \theta = \cos \theta$  and the Eq. (24) reduces to

$$K_E = 1 / \left( \frac{2}{\sqrt{(nK_N \sin \theta)^2 + (nK_V \cos \theta)^2}} + \frac{1}{K_h} \right) \quad (25)$$

Under compression, the effective stiffness of the haunch and anchor would be higher than that of the effective stiffness of the haunch and anchor assembly in tension as the force is transferred through bearing of the connection plate with concrete surface and through the shearing of the anchors. Based on the experimental observation of Genesisio (2012) the effective compression stiffness of the haunch and anchor assembly is 1.5 times that of effective tensile stiffness. Thus, in the case of haunch connection using post-installed anchors,  $\beta_1$  has to be evaluated using effective stiffness ( $K_E$ ) of both the haunch and anchors against the stiffness of haunch ( $K_h$ ) alone in the case of integral haunch connection.

For haunch connection using post-installed anchors, the effective stiffness of the haunch and anchor groups is primarily governed by the stiffness of the anchor groups rather than by the stiffness of haunch and this is well explained below with an assumed stiffness for anchor groups. The normal and shear stiffness of the anchor group is assumed as 200 kN/mm and 80 kN/mm respectively. For the stiffness of haunch of 250 kN/mm, the effective stiffness evaluated from Eqs. (23) and (25) are found to be 90 kN/mm and 58 kN/mm respectively. Similarly, for the stiffness of haunch of 1000 kN/mm, the effective stiffnesses evaluated from Eqs. (23) and (25) are found to be 123 kN/mm and 71 kN/mm respectively. The increase in haunch stiffness by four times (i.e., from 250 to 1000 kN/mm) increased the effective stiffness by 36% and 22% according to Eqs. (23) and (25) respectively. Thus, in the case of haunch connection with post-installed anchors, it is suggested to choose the stiffness of haunch slightly higher than the value of normal stiffness of the anchor groups.

### 2.3 Parametric study to evaluate influence of various geometric parameters on steel haunch factors $\beta_1$ and $\beta_2$

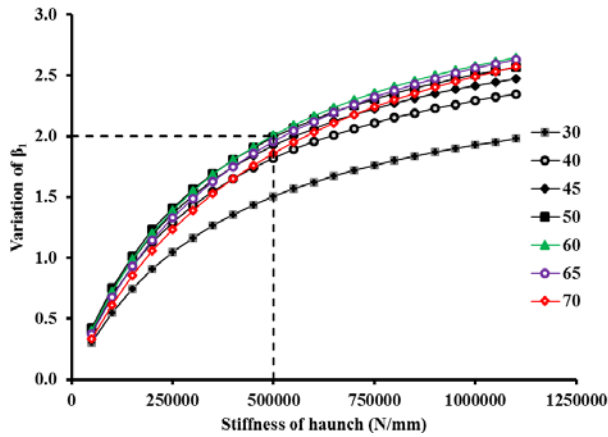
It is essential to understand the influence of geometrical parameters, namely, stiffness of haunch, orientation angle of

Table 1 Geometric and material properties of beam-column sub-assembly considered for parametric study

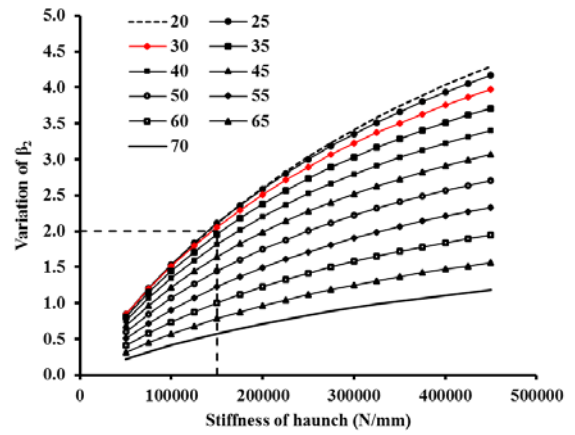
Parameter	Value
Length of beam up to contra-flexure point ( $L_c$ )	1550 mm
Height of column ( $H_c$ )	3500 mm
Width of beam ( $b$ )	300 mm
Depth of beam ( $d$ )	400 mm
Width of column ( $b_c$ )	300 mm
Depth of column ( $h$ )	300 mm
Young's modulus of Concrete ( $E_c$ )	31623 N/mm <sup>2</sup>
Young's modulus of steel ( $E_s$ )	$2 \times 10^5$ N/mm <sup>2</sup>

the haunch ( $\theta$ ), effective moments of inertia of beam ( $I_B$ ) and column ( $I_C$ ) segments, length of beam ( $L_B$ ) and height of column ( $H_C$ ) on steel haunch force factors  $\beta_1$  and  $\beta_2$  for evolving sizes of strengthening/upgradation strategy. In order to understand the influence of various geometric parameters on the values of  $\beta_1$  and  $\beta_2$  under combined gravity and lateral loads, a parametric study is carried out on the exterior beam-column sub-assembly retrofitted with steel haunch. The material and geometric properties considered for carrying out the parametric study are given in Table 1.

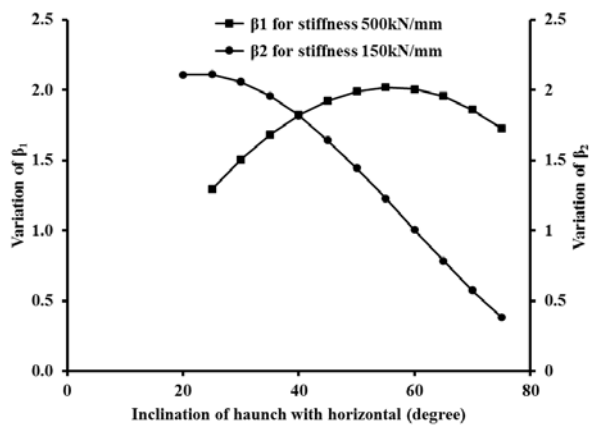
The paramount parameters governing the values of  $\beta_1$  and  $\beta_2$  are the stiffness and the orientation angle of the haunch with the horizontal. The effective moments of inertia of beam and column segments are assumed as  $0.5I_{gb}$  and  $0.9I_{gc}$  respectively, where  $I_{gb}$  and  $I_{gc}$  are gross moment of inertia of beam and column respectively. The variation of  $\beta_1$  and  $\beta_2$  with stiffness and orientation angle of the haunch is evaluated using the formulation presented in the preceding Section 2.2 and is depicted in Figs. 3(a) and 3(b) respectively. From Fig. 3(a), it may be observed that as the angle of orientation of the haunch and stiffness of the haunch increase, the value of  $\beta_1$  increases up to an angle of 60 degree and afterwards the value of  $\beta_1$  decreases. It could also be observed that the value of  $\beta_1$  is maximum for the orientation angles of haunch between 45-60 degree with the horizontal. Whereas,  $\beta_2$  is maximum for the orientation angles of haunch between 20-25 degree. The value of  $\beta_1$  is found to be greater than 2 for the stiffness of haunch greater than or equal to 5,00,000 N/mm for the orientation angle between 50-60 degree. The value of  $\beta_2$  is greater than 2 for the stiffness of haunch of 150000 N/mm for the orientation angle between 20-30 degree. From Figs. 3(a) and (b), it may be noted that for haunch orientation angle of 45-degree, providing haunch stiffness greater than 5,50,000 N/mm would result in the beam shear higher than the shear due to lateral load and haunch stiffness greater than 2,00,000 N/mm would result in the column shear greater than the shear due to lateral load. Hence, for the given sub-assembly, it is not desirable to go for stiffness higher than 2,00,000 N/mm. Thus, choosing higher stiffness of haunch alone does not result in the effective upgradation solution rather it is essential to choose appropriate stiffness of haunch in order to avoid undesirable forces on beam and column segments. Thus, Figs. 3(a) and (b) provide valuable



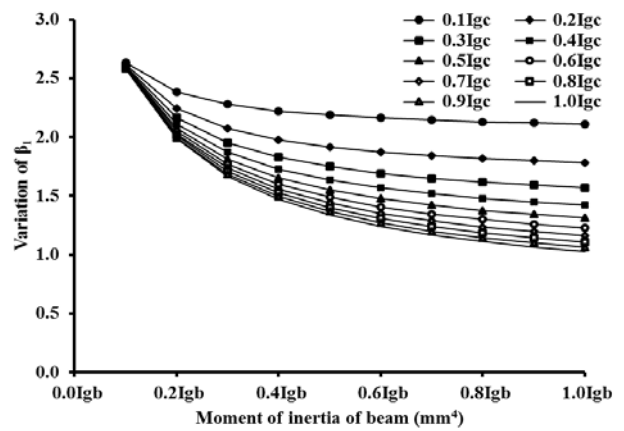
(a) Variation of  $\beta_1$  with stiffness and orientation of haunch



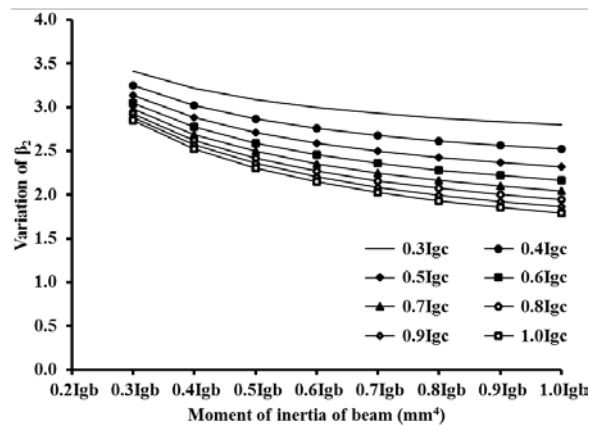
(b) Variation of  $\beta_2$  with stiffness and orientation of haunch



(c) Variation of  $\beta_1$  and  $\beta_2$  with angle of inclination of haunch



(d) Variation of  $\beta_1$  with moment of inertia of beam and column segments



(e) Variation of  $\beta_2$  with moment of inertia of beam and column segments

Fig. 3 Variation of  $\beta_1$  and  $\beta_2$  with stiffness and orientation of haunch; and moment of inertia of beam and column segments

insight and information for dimensioning of steel haunch. Fig. 3(c) shows variation of  $\beta_1$  and  $\beta_2$  with orientation angle of the haunch for the selected stiffness values.

The variation of  $\beta_1$  and  $\beta_2$  with effective moments of inertia of beam and column segments for the selected haunch orientation angle of 45 degree, diameter of 30 mm and length of 565.69 mm is shown in Figs. 3(d) and (e) respectively. The effective moments of inertia of beam and column segments are expressed as fraction of gross moment

of inertia of beam ( $I_{gb}$ ) and column ( $I_{gc}$ ). It is important to highlight the fact that the values of both  $\beta_1$  and  $\beta_2$  are sensitive to the effective moment of inertias of beam and column segments as shown in Figs. 3(d) and (e) respectively. It could be observed from these figures that the values of both  $\beta_1$  and  $\beta_2$  increase with the decrease in effective moment of inertia (representing the scenario of cracked sections), particularly at the lower values of moment of inertia of both beam and column sections. The

values of  $\beta_1$  and  $\beta_2$  increase more with decrease in effective moment of inertia of beam rather than that of the column. This also gives very important insight that haunch force is less till first crack load and the force transfer to the haunch increases with the increase in cracking. The moment of inertia of the section corresponding to the yielding of reinforcement is recommended for the design of haunch as effective moment of inertia.

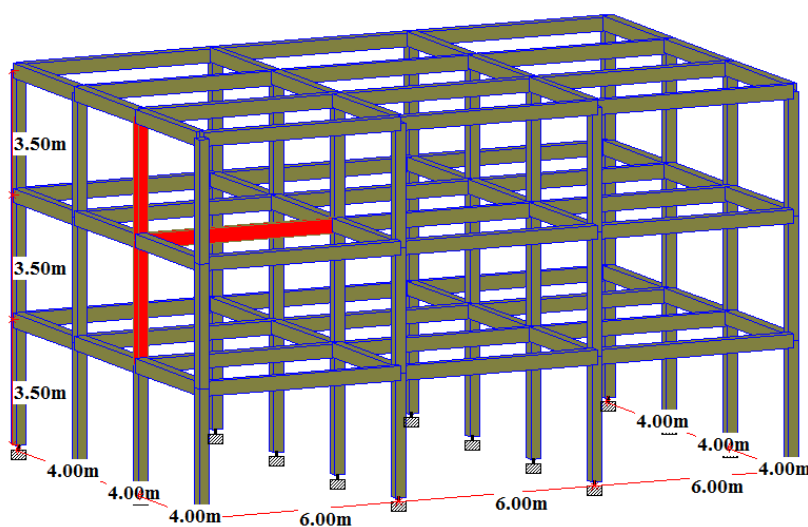
The increase in length of the beam would increase the value of  $\beta_1$ . The increase in the length of beam increases the flexibility of the beam which in turn throws larger forces into the haunch as relative stiffness increases. Similarly, the value of  $\beta_2$  also increases with the increase in column height. The parametric study carried out above is also valid for haunch connections with post-installed anchors provided the effective stiffness of haunch and anchor assembly is taken in the place of stiffness value of haunch.

The parametric study is intended to understand the influence of various parameters on the force flow through alternate force path i.e., haunch. Further, choosing inappropriate stiffness of haunch would result in undesirable beam shear. The nonlinearity can be considered in the evaluation of haunch force factor by using the cracked moment of inertia of beam corresponding to the yielding of beam reinforcement. If yielding of beam reinforcement occurs first, before other failure modes, haunch force is restricted by the beam tip load corresponding to the flexural capacity of beam or yield strength of the steel haunch. At present state of knowledge, it is recommended to choose a value less than 2 for both  $\beta_1$  and  $\beta_2$  and also strengthening scheme could be designed in such a way that flexural capacity of beam is reached first.

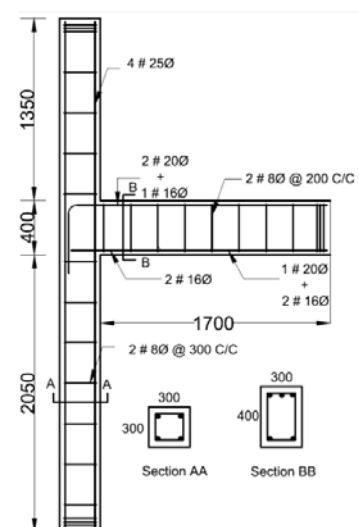
### 3. Details of GLD exterior beam column sub-assembly and SHUS

A full scale exterior beam-column sub-assembly of a typical three storied RC framed building representing old

Indian construction is considered in the present study as shown in Fig. 4(a). 3D numerical simulation of the building frame is carried out and analysed for combination of dead load and live load to obtain the design forces in beam and column segments of the sub-assembly considered in the present study. The frame is designed and detailed according to Indian Standard IS 456 (2000) and SP 34 (1987). The cross sectional dimensions adopted for beam and column sections are 300 mm  $\times$  400 mm and 300 mm  $\times$  300 mm respectively and the reinforcement details of the specimen are shown in Fig. 4(b). The length of beam is arrived based on the point of contra-flexure under the action of combined gravity loads and lateral loads. The lengths of column segments above and below the joint are arrived according to the proportioning of moments at the joint for the combination of loads. The general dimensions of beam-column sub-assembly are as follows: height of column segment is 3800 mm and length of beam segment is 1700 mm. Two such specimens are cast and one of them is control GLD specimen (SP1) and the other GLD is used for steel single haunch upgradation strategy (SHUS) (SP1-U1). It is important to mention here that the beam bottom bars in gravity load designed specimen project straight into the joint region. The specimens are instrumented extensively by affixing strain gages on reinforcement bars in the disturbed regions of the beam-column sub-assembly. As representation of majority of existing RC framed buildings (3-5 stories), grade of concrete chosen for the study is M30 (i.e., 30 Mpa). The standard deviation for M30 grade concrete is 5.0 MPa. The target mean strength of concrete mix is equal to the characteristic strength plus 1.65 times the standard deviation. Thus, the target mean strength of M30 grade concrete is 38.25 MPa. Based on concrete mix design, concrete mix of 1:1.695:3.013 proportions and with water cement ratio of 0.5 is used for casting of the specimens. The specimens are cast and cured for 28 days using wet curing. The concrete cylinders that are cast along with the specimens are tested and the average compressive strength and split tensile strength of concrete are presented in Table



(a) Exterior beam-column sub-assembly considered for study



(b) Geometrical and reinforcement details of specimen

Fig. 4 Details of building and beam-column sub-assembly chosen for study

Table 2 Strength parameters of concrete

Specimen ID	Average cylinder compressive strength (N/mm <sup>2</sup> )	Average split tensile strength (N/mm <sup>2</sup> )
SP1	41.34	3.7
SP1-U1	38.71	3.29

Table 3 Material properties of steel reinforcement

Diameter of reinforcement (mm)	Yield strength of steel (N/mm <sup>2</sup> )
8	527
16	545
20	520
25	535

2. The reinforcement steel used in this study is high strength deformed bars of grade Fe500D conforming to IS:1786-2008. The material properties of steel used in the present study are given in Table 3.

### 3.1 Upgradation of GLD specimen using SHUS

From the analytical studies presented in the preceding sections, for SHUS, the value of  $\beta_1$  is maximum is for the orientation angles between 45-60 degree. Hence, orientation angle of 45 degree with the horizontal is chosen for the present study. The haunch would act as prop and aids in the beam bottom bars to develop which avoids the anchorage failure of beam bottom reinforcement. For 16 mm diameter bars at bottom of the beam, development length is 35 times diameter of the rebar and thus 560mm is needed to prevent anchorage failure. Hence, the haunch is connected at distance of 400 mm from the face of the joint and the rebar projects nearly 210 mm into the column. So that, SHUS would be able to prevent the anchorage failure of the reinforcement. The haunch is designed as yielding haunch at the load corresponding to yielding of beam top reinforcement. A mild steel haunch of 30 mm diameter is chosen to cater for the load corresponding to beam top reinforcement. The haunch connection is established by means of post-installed anchors. Thus, for the chosen dimensions of the haunch, haunch force factor  $\beta_1$  is evaluated analytically using Eq. (21) with the effective haunch stiffness. The effective moment of inertia of the beam sections are obtained from the curvature analysis of the section at the location of haunch at yielding of steel reinforcements. The effective moment of inertia of column section is assumed as 0.8 times of its gross moment of inertia. The stiffness of the anchors in tension and shear are obtained from ETA 05/255, 2016. The stiffness of the anchor in cracked concrete is evaluated as 0.45 times that in uncracked concrete (Sharma 2013). The value of  $\beta_1$  is evaluated analytically using Eq. (21). The maximum and minimum values of  $\beta_1$  are obtained for the effective stiffnesses of haunch and anchorage system ( $K_E$ ) evaluated vide Eqs. (23) and (25) respectively. The values of  $\beta_1$  estimated analytically are shown in the Table 4. The actual

Table 4 Values of  $\beta_1$  evaluated analytically

Values of $\beta_1$			Remark
Maximum	Minimum	Average	
1.2	0.95	1.075	Haunch under tension (+ve cycle)
1.16	0.92	1.04	Haunch under compression (-ve cycle)

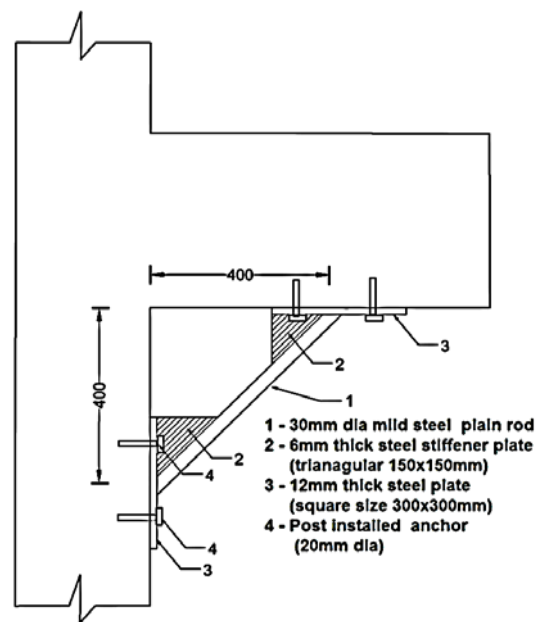
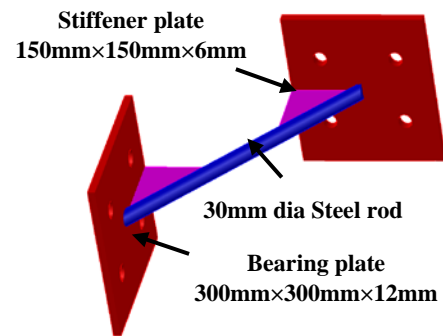


Fig. 5 Details of steel haunch upgradation system

value of  $\beta_1$  would be in between the analytically estimated values. It is expected that the provision of haunch avoids brittle failure of beam bottom bars, delay the joint shear damage and the damage is partially directed towards the beam.

The unsupported length of the haunch is maintained less than 5 times the diameter of the haunch by welding triangular stiffener plates of size 150 mm × 6 mm at each end as shown in Fig. 5. Steel Haunch system adopted in the present study consists of steel rod welded to steel base plates and the rod is stiffened by welding triangular stiffener plates to steel rod at both ends as shown in the Fig. 5. Prior to the installation of haunch, the rebars in the beam and column segments are located using Ground Penetration

Radar. Then holes are drilled on the steel base plates of the haunch system in such a way that rebars do not interfere with the drilling of anchor holes. Hilti HAS-E bolts of 20 mm diameter and 170 mm embedment length with HVU adhesive are used for anchoring the haunch to the beam-column sub-assembly. Firstly, holes of 24 mm diameter and 170 mm embedment length are drilled into the concrete using drilling machine. Holes are cleaned properly using air blower/compressor so as to remove dust particles present in the hole so that perfect bond between the adhesive and concrete can be achieved. For providing the anchorage to the bolts, HVU adhesive capsule is inserted into the hole and then bolt is forced to punch through the capsule using drilling machine. The HAS-E Bolt has a special groove on its tip to pierce through the capsule thereby providing bond between anchor and parent material. After the desired curing time, haunch is connected to the beam and column segments by tightening the nuts of anchor bolts against base plates of haunch system. Tightening of the nuts of anchor bolts against base plates is carried out using a torque wrench with a torque of approximately 150 N-m. The entire exercise of upgradation of beam-column sub-assembly is done with post-installed anchors with a view to demonstrate the efficacy of this practical upgradation strategy for seismic upgradation of deficient existing structures. For successful implementation of seismic retrofit using post-installed anchors, the choice of anchors is very important. It is essential to take into account the factors such as cracking and low strength of concrete during the selection of anchors. For cracked concrete with crack width more than 1mm, undercut anchors are suitable and qualified adhesive anchors and torque based expansive anchors are acceptable (Balbuena *et al.* 2011). Furthermore, chemical anchors could be employed for low strength concrete provided if the free edge distance and embedment depth are 15 times diameter of the anchor (Yilmaz *et al.* 2013).

#### 4. Experimental investigations on GLD and upgraded GLD specimens

The test specimens viz., GLD specimen (SP1) and upgraded GLD (SP1-U1) specimen with SHUS using post-

installed anchors are also instrumented with LVDTs (linear variable displacement transducers), which were mounted on the beam and the column segments to measure deflections along the length of beam and column segments. The test setup is arranged on the test floor so that the beam-column joint is positioned horizontally parallel to the test floor and the cyclic load is applied in the plane of the test floor. The schematic view of the test set-up, positioning of the specimen in the actual test setup and instrumentation adopted are shown in the Figs. 6(a) and (b) respectively.

An axial load of 300 kN is applied to the column by hydraulic jack at one end of the column against the reaction block at the other end. The level of axial load in column is arrived by carrying out analysis of the global system of the three-storied three-bay building. The lateral load is applied on the beam tip in displacement control mode using 250 kN actuator, according to the load history shown in Fig. 7. Reverse cyclic load is applied in terms of drift ratio (%) of the component and the drift is calculated as per Eq. (26).

$$\text{Drift ratio (\%)} = (\Delta/l_b) \times 100 \quad (26)$$

Where,  $\Delta$  and  $l_b$  are the applied displacement at the beam tip and the length of the beam from column face to the point of application of the displacement increment respectively. The load is applied at the beam tip by gradually increasing cyclic displacements in multiples of

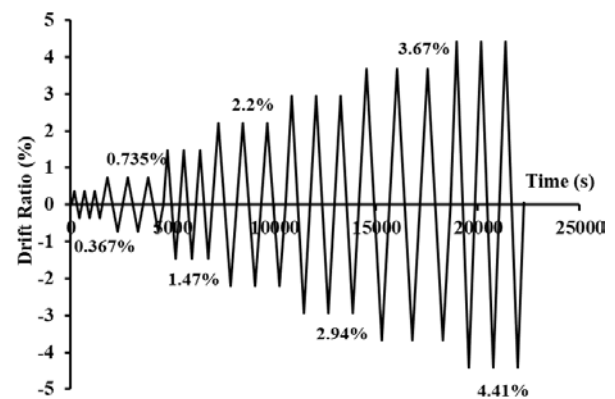
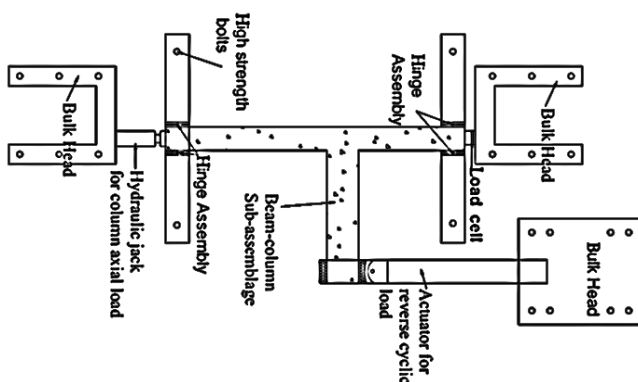


Fig. 7 Reverse cyclic loading history



(a) Schematic view of test setup



(b) Actual test setup and instrumentation adopted for experimental investigation

Fig. 6 Schematic and actual test setup

12.5 mm i.e., drift ratio of 0.735%. i.e., 0.3675 % (6.25 mm), 0.735% (12.5 mm), 1.47% (25 mm), 2.2% (37.5 mm), 2.94% (50 mm), 3.675% (62.5 mm), 4.41% (75 mm). Three complete cycles are applied for each drift increment. Reverse cyclic displacements of equal magnitude are applied on the specimens at each drift ratio. Positive drift produces tension in the beam bottom and negative drift produces tension in beam top.

**5. Evaluation of comparative performance of GLD (SP1) and upgraded GLD (SP1-U1) specimens**

It is evident that specimen SP1 which is designed only for gravity loads, would exhibit poor seismic performance due to insufficient anchorage and inadequate reinforcement at beam bottom for seismic event. The enhancement in seismic performance of upgraded GLD specimen is evaluated by comparing the response of upgraded GLD specimen (SP1-U1) with that of the GLD (SP1) specimen in terms of seismic performance parameters, namely damage progression, load-displacement behavior, energy dissipation capacity, stiffness and global strength degradation. The details and discussion of results are presented in the following sections.

*5.1 Damage progression and ductility*

In GLD specimen (SP1), a prominent joint crack of

3 mm width is developed at the face of the column at positive drift ratio of 1.47% as shown in Fig. 8 due to anchorage failure of beam bottom reinforcement. At a drift ratio of +2.94%, width of the same crack has widened to 13 mm. Whereas in the case of upgraded GLD specimen (SP1-U1), at positive drift ratio of 1.47%, a prominent flexural crack is developed in the beam at the location of haunch as shown in Fig. 9. The flexural crack developed at haunch location is propagated up to the beam top. Thus, the damage is shifted to beam during the positive cycle of loading in the upgraded GLD specimen (SP1-U1) and thereby avoiding one of the brittle modes of failure i.e., anchorage failure of beam bottom reinforcement, as was present in the GLD specimen (SP1). Thus, the SHUS succeeded in partially redirecting the damage towards the beam in the positive cycle.

In GLD specimen SP1, upon drift increment beyond negative drift ratio of -1.47%, the damage shifted towards the joint region. As there is no transverse reinforcement, the shear resistance of joint completely relies on the diagonal strut mechanism. Due to insufficient anchorage of bottom beam bars into the joint, the strut mechanism could not be mobilized during positive cycles whereas this could be mobilized in the negative cycle. Hence, the joint shear cracks are developed and propagated as shown in Fig. 10 during negative cycles rather than in positive cycles. In the case of upgraded GLD specimen SP1-U1, in the negative cycles, damage started with flexural cracking at haunch-beam connection. At the drift ratio of -1.47%, shear cracks

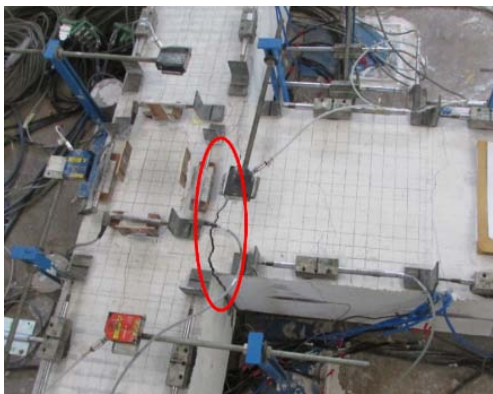


Fig. 8 Crack pattern at drift ratio of +1.47% for SP1

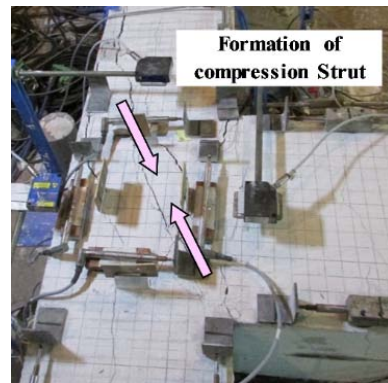


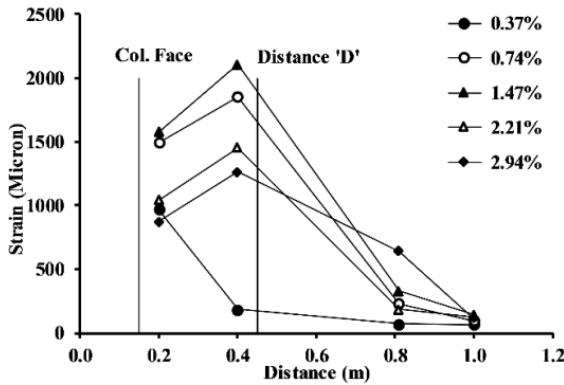
Fig. 10 Crack pattern of SP1 at drift ratio of -2.94%



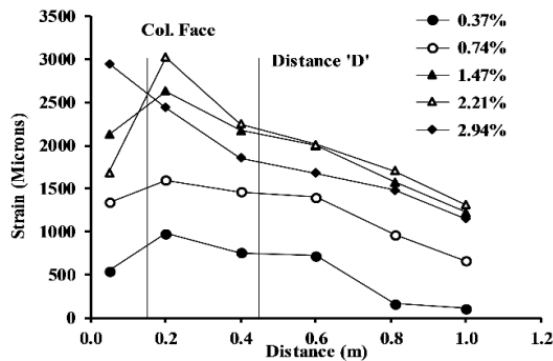
Fig. 9 Crack pattern observed at drift ratio of +1.47% for SP1-U1



Fig. 11 Crack pattern of SP1-U1 at drift ratio of -2.94%



(a) Strain profile of beam bottom bars of SP1 during positive drift cycles



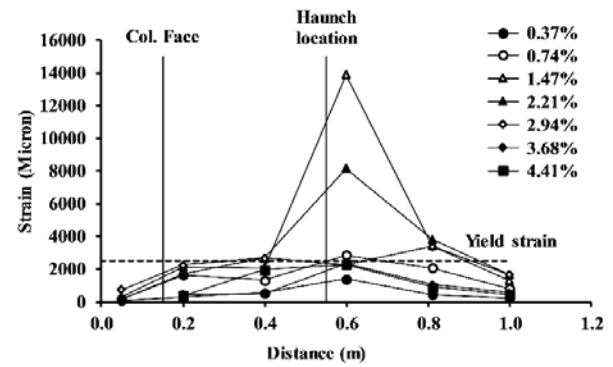
(b) Strain profile of beam top bars of SP1 during negative drift cycles

Fig. 12 Strain profile of beam reinforcements in SP1

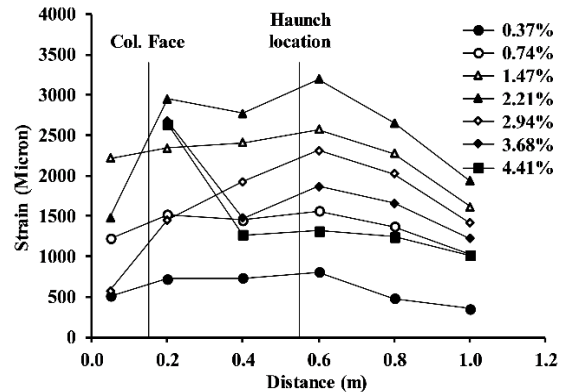
appeared along the diagonal of the joint. Fig. 11 shows crack pattern of SP1-U1 at the drift ratio of -2.94%. The diagonal crack propagated into the column region with further drift increment in negative cycles. At the final stage of loading, i.e., at negative drift ratio of -4.41%, joint crack is widened and propagated into the zone beyond the 'D' region in column. The upgraded GLD specimen SP1-U1 sustained larger drift cycles when compared with the control GLD specimen SP1. In the negative cycles, damage started with flexural cracking at haunch-beam connection but finally damage is manifested in the form of joint shear damage.

In control GLD specimen SP1, during positive drift cycles of loading, the strain values of beam bottom bars are well below the yield strain of steel throughout the length of the beam as can be seen from Fig. 12(a). In GLD specimen SP1, at the drift ratio of -1.47%, yielding of beam reinforcement could be seen from strain profile of beam top bars presented in Fig. 12(b). The strains increase over a distance D from the face of the joint in beam top bars up to the drift ratio of -2.2%. Beyond this drift ratio, the strains dropped along length of the beam as can be seen from Fig. 12(b). The global strength degradation behavior is observed due to the growth and propagation of the diagonal shear cracks in the joint region.

From the strain profile of beam bottom reinforcement of upgraded GLD specimen SP1-U1 as shown in Fig. 13(a), it is observed that the maximum strain is developed at



(a) Strain profile of beam bottom bars of SP1-U1 during positive drift cycles



(b) Strain profile of beam top bars of SP1-U1 during negative drift cycles

Fig. 13 Strain profile of beam reinforcements in SP1-U1

distance of nearly 0.6 m from the center line of column i.e., at the location of haunch. The strain level in reinforcement at this location is high due to the widening of flexural crack at drift ratio of 1.47%. Further, it could be observed that there is spreading of yield zone on either side of haunch location i.e., between 0.4 m to 0.8 m from the center line of the column. Thus, the presence of haunch prevented the anchorage failure of beam bottom reinforcement bars which is one of the critical issues of gravity load designed sub assemblage with straight beam bar anchorage. It could also be observed from Fig. 13(b) that the yielding of reinforcement happened at drift ratio of -1.47% at a distance of 0.6 m from the center line of the column, i.e., at the haunch location. Even after the appearance of the diagonal shear cracks in the joint region at the drift ratio of -1.47%, the beam strain values tend to increase up to the first cycle of -2.2% drift ratio due to the reduction of shear demand on the joint due to alternate force path provided by the haunch which resulted in the improvement in load carrying capacity in the negative cycle compared with SP1. At drift ratio of -2.94%, global strength degradation is observed due to the damage progression in the form of joint damage by widening of joint shear cracks. This is reflected by the drop in strain at the drift ratio of -2.94% along the length of the beam. It is observed that there is delay in joint shear damage and improvement in load carrying capacity during negative cycles in the case of upgraded GLD specimen SP1-U1.

### 5.2 Load – Displacement hysteresees

The single steel haunch upgradation improved the hysteretic behavior of upgraded GLD beam-column sub-assembly SP1-U1 to large extent as shown in Fig. 14.

The GLD specimen showed poor hysteretic performance due to anchorage failure of beam bottom reinforcement which could be witnessed at the positive drift ratio of +1.47% as sudden load drop and the progressive load drop

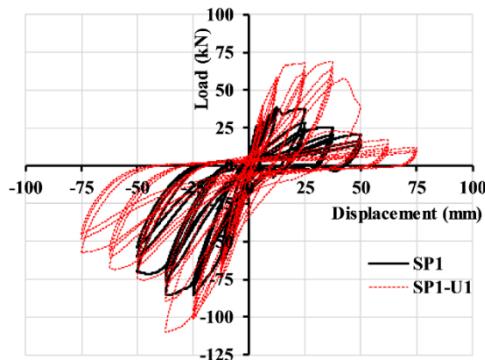


Fig. 14 Load versus Displacement Hysteresis of the specimens SP1 and SP1-U1

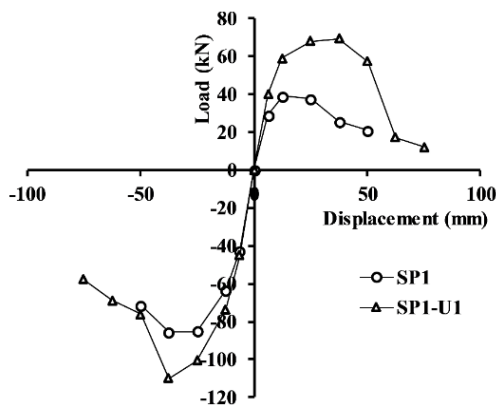


Fig. 15 Load displacement envelopes of the specimens SP1 and SP1-U1

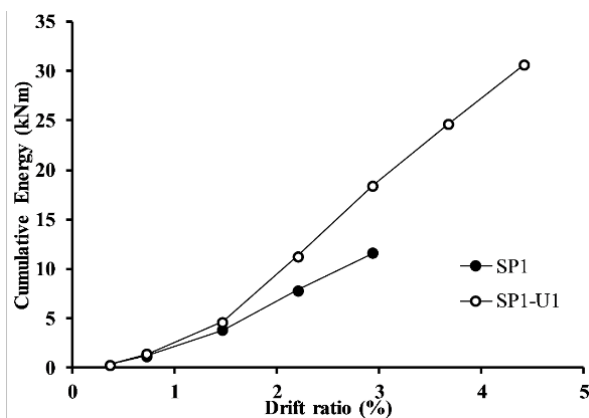


Fig. 16 Cumulative energy dissipated by control GLD and upgraded specimens

is observed with the drift increments. Upgraded GLD specimen SP1-U1 showed phenomenal improvement in the load carrying capacity and also sustained larger displacements compared with to the control GLD specimen SP1.

The load carried during the negative displacement cycles is more compared with that during positive displacement cycles as the reinforcements at beam top and bottom are not equal. It is noted from load-displacement envelopes presented in Fig. 15 that there is a remarkable enhancement in the maximum load carried by upgraded GLD specimen (SP1-U1) compared with that of the control GLD specimen (SP1) for each and every drift ratio. The maximum load carried by SP1-U1 during the positive and negative cycles is 69 kN and 110 kN respectively against the maximum load of 39 kN and 85 kN respectively carried by SP1 during positive and negative displacement cycles. The maximum load carried by SP1-U1 is 1.77 and 1.29 times that of SP1 during positive and negative cycles respectively. Haunch reduces the shear demand on the joint and improves the load carrying capacity in the negative cycle. Thus, there is delay in joint shear damage and improvement in load carrying capacity during negative cycle in the case of upgraded specimen. It is also observed that load is increased till the drift ratio of  $\pm 2.2\%$  (37.5 mm) in upgraded GLD specimen (SP1-U1) whereas load is increased till the drift ratio of  $+0.735\%$  (12.5 mm) and  $-2.2\%$  (37.5 mm) in control GLD specimen. Thus, from the above it can be concluded that the single steel haunch upgradation strategy is a very good candidate for seismic upgradation of existing GLD RC structures in the regions of moderate seismic risk as it demands for higher load carrying capacity rather than a ductile response and also preventing brittle anchorage failure of reinforcement bars.

### 5.3 Energy dissipation

Energy dissipation is one of the vital seismic performance parameters. The energy imparted by earthquake has to be dissipated globally by the structure as a whole. This could be achieved only if the individual components are capable of dissipating the energy imparted to them. Comparison of cumulative energy dissipated by control GLD (SP1) and upgraded GLD specimens (SP1-U1) is shown in Fig. 16. The GLD specimen SP1 exhibited poor energy dissipation due to the anchorage failure. Both control GLD (SP1) and upgraded GLD (SP1-U1) specimens dissipated same energy up to the drift ratio of 0.734% till the development of flexural cracking in the beam. Beyond this drift ratio, the energy dissipated by control GLD specimen SP1 is smaller compared with that of upgraded GLD specimen SP1-U1. The cumulative energy dissipated by SP1-U1 up to the drift ratio of 2.94% (final stage of SP1) is 1.58 times that of SP1. The maximum cumulative energy dissipated by GLD and upgraded GLD specimens are found to be 11.65 kNm and 30.63 kNm respectively. Thus, the cumulative energy dissipated by upgraded GLD specimen SP1-U1 is 2.63 times that of control GLD specimen SP1. This remarkable improvement in the energy dissipation by upgraded GLD specimen SP1-U1 is due to the improved load carrying capacity, prevention of anchorage failure of beam bottom reinforcements bars and sustaining larger drift

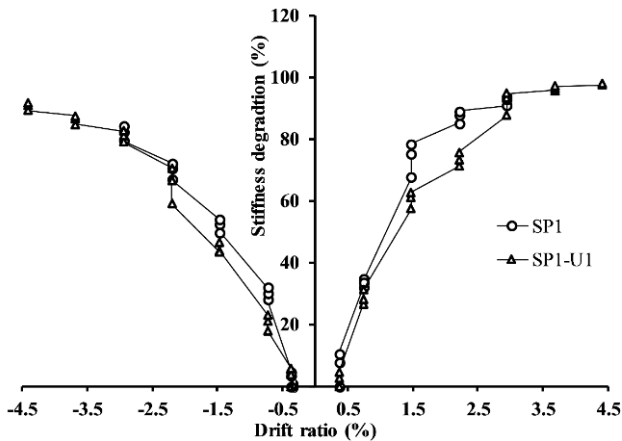


Fig. 17 Stiffness degradation of GLD (SP1) and upgraded GLD (SP1-U1) specimens

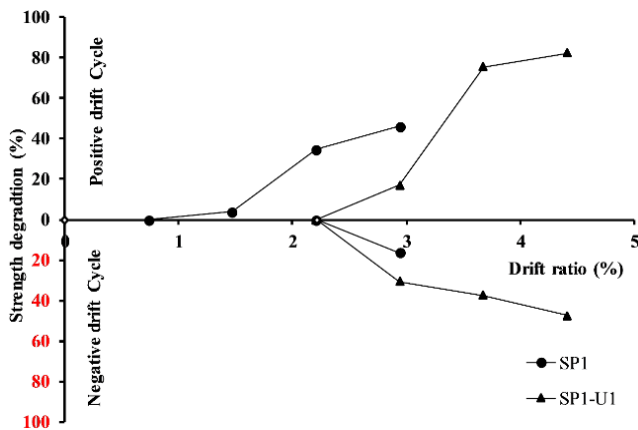


Fig. 18 Global strength degradation of GLD (SP1) and upgraded GLD (SP1-U1) specimens

cycles. This enhanced energy dissipation capacity of upgraded GLD specimen demonstrated the effectiveness of SHUS for seismic upgradation of deficient existing RC structures.

#### 5.4 Stiffness degradation

The stiffness degradation is expressed as the percentage degradation in stiffness of all cycles of each drift increment with respect to the stiffness of first cycle of initial drift ratio. The stiffness degradation undergone by both control GLD (SP1) and upgraded GLD (SP1-U1) specimens is shown in Fig. 17. The specimens SP1 and SP1-U1 have undergone almost nearly the same amount of stiffness degradation in both positive and negative cycles till the drift ratio of 0.367%. The specimen SP1 has undergone drastic stiffness degradation i.e., 32% at drift ratio of +0.735% and 68% at drift ratio of +1.47%, due to the anchorage failure of beam bottom reinforcement bars at drift ratio of +1.47%. From the drift ratio of 0.735% till the drift ratio of 2.94% (up to the maximum displacement sustained by SP1), the stiffness degradation of SP1-U1 is smaller than that of SP1 in both positive and negative cycles. At drift ratio of  $\pm 2.2\%$ , the stiffness degradation in first cycle of SP1 is 16% and 12% greater than that in the first cycle of SP1-U1 in

positive and negative cycles respectively. In the upgraded GLD specimen, towards the larger drift ratios (after  $\pm 2.2\%$ ) wide crack had developed at the haunch-beam connection during the positive cycle and excessive joint cracking is witnessed during the negative cycles leading to large stiffness degradation. The stiffness degradation of SP1-U1 is 98% and 91% at final stage (at drift ratio of 4.41% which is much higher compared with final drift ratio of 2.94% in the case of SP1) in the positive and negative cycles respectively. Further, it is noted that the stiffness degradation during negative cycles is relatively smaller compared with that during positive cycles due to the proper anchorage of beam reinforcement and larger area of reinforcement at the beam top in both the specimens.

#### 5.5 Global strength degradation

Cyclic strength degradation i.e., the strength degradation with subsequent cycles with drift increment, of GLD (SP1) and upgraded GLD specimens (SP1-U1) is presented in Fig. 18. For arriving at the strength degradation after reaching the maximum load in the positive or negative drift cycles, the strength degradation during the first cycle of subsequent drift cycles with reference to that of the maximum load is calculated. From Fig. 18, it may be noted that the global strength degradation begins after the drift ratio of +0.735% in the case of control GLD specimen SP1 whereas the same has happened after the drift ratio of +2.2% in the upgraded GLD specimen SP1-U1. This depicts the phenomenal shift in the global strength degradation behavior observed in the upgraded GLD specimen SP1-U1 with the drift increment, particularly in the positive cycle. The strength degradation for SP1 is found to be 46% (from 39 kN at 0.735% to 21 kN at 2.94%) at the drift ratio of +2.94%. At the same drift ratio, strength degradation for SP1-U1 is only 17% (from 69 kN at 2.2% to 57 kN at 2.94%). The upgraded GLD specimen SP1-U1 exhibited superior performance in positive drift cycles w.r.t strength degradation.

During negative cycles of loading, the global strength degradation of both GLD and upgraded GLD specimens is observed after the drift ratio of -2.2%. At drift ratio of -2.94%, the strength degradation of GLD specimen SP1 is 16% (i.e., load dropped from 85.5 kN at -2.2% to 71 kN at -2.94%) and that of upgraded specimen SP1-U1 is 30% (i.e., load dropped from 109 kN at -2.2% to 76 kN at -2.94%). Even though there is an improvement in load carrying capacity of SP1-U1 in comparison with that of SP1 during the negative cycles, the strength degradation of SP1-U1 is higher than that in SP1 at the drift ratio of -2.94% (final stage of SP1 specimen). This is due to the compression yielding followed by buckling of haunch thereby making it less effective and resulting in the load drop from the improved load carrying capacity to the capacity corresponding to degraded joint strength. By restraining the buckling of the haunch, better performance during negative cycles can be obtained.

## 6. Conclusions

In the present study, the focus is on formulation of a

practical and non-invasive seismic upgradation strategy for existing GLD RC structures. Steel single haunch upgradation strategy (SHUS) is chosen for the upgradation of GLD exterior beam-column sub-assembly of a typical three storied RC building. The primary focus of the upgradation is to prevent the anchorage failure of beam bottom reinforcement bars of GLD specimen, delaying the joint failure mechanism as far as possible and to attempt for redirecting the failure towards the beam to the extent possible under seismic event. Formulations are presented to aid in proportioning and positioning of the haunch for the most practical case of implementation of single haunch upgradation using post-installed anchors. From the experimental investigations carried out in this study, it is evident that the anchorage failure of the beam bottom bars of GLD specimen is prevented and yielding of reinforcement had happened at haunch-beam connection during the positive cycle through the implementation of SHUS. During the negative cycle, the joint shear failure is delayed and an improvement in the load carrying capacity of the upgraded GLD beam-column sub-assembly is observed. Further, by adopting SHUS for retrofitting of GLD beam-column sub-assembly, the damage progression is partially directed towards the beam. It is found that the maximum load carrying capacity of upgraded GLD specimen SP1-U1 during the positive and negative cycles is 69 kN and 110 kN respectively against the maximum load carrying capacity of 39 kN and 85 kN of control GLD specimen SP1 during the positive and negative cycles respectively. The maximum load carried by SP1-U1 is 1.77 and 1.28 times that of SP1 in positive and negative drift cycles respectively. Thus, remarkable improvement in the maximum load carrying capacity was observed in the case of SP1-U1 compared with SP1 particularly in positive displacement cycles. A tremendous improvement in the energy dissipation to the tune of 2.63 times that of SP1 is observed in SP1-U1. It can be concluded that SHUS is a very good candidate for upgradation of existing GLD RC structures in the regions of moderate seismic risk as it possesses good energy dissipation. This study provided a viable non-invasive retrofit scheme for seismic upgradation of deficient GLD RC structures.

## Acknowledgments

The authors express their heartfelt thanks to the support rendered by the staff members of Advanced Concrete Testing and Evaluation Laboratory and Structural Testing Laboratory of CSIR-SERC during the experimental investigations of the beam-column sub-assemblies.

## References

- Adam, J.M., Giménez, E. and Calderón, P.A. (2008), "Experimental study of beam-column joints in axially loaded RC columns strengthened by steel angles and strips", *Steel Compos. Struct., Int. J.*, **8**(4), 329-342.
- Adibi, M., Marefata, M.S., Arani, K.K. and Zare, H. (2017), "External retrofit of beam-column joints in old fashioned RC structures", *Earthq. Struct., Int. J.*, **12**(2), 237-250.
- Akguzel, U. and Pampanin, S. (2012), "Recent Developments in Seismic Strengthening of RC Beam-Column Joints with FRP Materials", *Proceedings of the 15th World Conference on Earthquake Engineering*, Lisbon, Portugal.
- Aycardi, L.E., Mander, J.B. and Reinhorn, A.M. (1994), "Seismic resistance of reinforced concrete frame structures designed only for gravity loads: Experimental performance of sub-assemblies", *ACI Struct. J.*, **91**(5), 552-563.
- Balbuena, G., Gramaxo, J. and Kunz, J. (2011), "Design of Post-installed Anchors for Seismic Actions", *Proceedings of the Ninth Pacific Conference on Earthquake Engineering Building an Earthquake-Resilient Society*, Auckland, New Zealand
- Bansal, P.P., Kumara, M. and Darb, M.A. (2016), "Retrofitting of exterior RC beam-column joints using ferrocement jackets", *Earthq. Struct., Int. J.*, **10**(2), 313-328.
- Bokey, P.B. and Pajgade, P.S. (2004), "Lessons from Jan, 26, 2001 Gujarat (India) Earthquake", *Proceedings of the 13th World Conference on Earthquake Engineering*, Vancouver, Canada, Paper No. 1874.
- Bracci, J.M., Reinhorn, A.M. and Mander, J.B. (1995), "Seismic resistance of reinforced concrete frame structures designed for gravity loads: performance of structural system", *ACI Struct. J.*, **92**(5), 597-609.
- Campione, G., Cavaleri, L. and Papia, M. (2015), "Flexural response of external R.C. beam-column joints externally strengthened with steel cages", *Eng. Struct.*, **104**, 51-64.
- Dogan, E. and Opara, N.K. (2003), "Seismic Retrofit with Continuous Slurry-Infiltrated Mat Concrete Jackets", *ACI Struct. J.*, **100**(6), 713-723.
- El-Amoury, T. and Ghobarah, A. (2002), "Seismic rehabilitation of beam-column joint using GFRP sheets", *Eng. Struct.*, **24**, 1397-1407.
- European Technical Assessment (2016), ETA-05/0255 of 19 January 2016.
- Fakharifar, M., Sharbatdar, M.K., Lin, Z., Dalvand, A., Sivandi-Pour, A. and Chen, G. (2014), "Seismic performance and global ductility of RC frames rehabilitated with retrofitted joints by CFRP laminates", *Earthq. Eng. Vib.*, **13**, 59-73.
- Genesio, G. (2012), "Seismic Assessment of RC Exterior Beam-Column Joints and Retrofit with Haunches Using Post-Installed Anchors", Doctor of Philosophy Thesis; University of Stuttgart.
- Gergely, J., Pantelides, C.P. and Reaveley, L.D. (2000), "Shear Strengthening of RCT-Joints Using CFRP Composites", *J. Compos. Constr.*, **4**, 56-64.
- Ghobarah, A. and Said, A. (2002), "Seismic rehabilitation of beam-column joints using FRP laminates", *J. Earthq. Eng.*, **5**(1), 113-129.
- Goltz, J. (1994), "The Northridge, California Earthquake of January 17, 1994: General Reconnaissance Report", Technical Report NCEER-94-0005; National Center for Earthquake Engineering Research.
- Hadi, M.N.S. and Tran, T.M. (2014), "Retrofitting non-seismically detailed exterior beam-column joints using concrete covers together with CFRP jacket", *Constr. Build. Mater.*, **63**, 161-173.
- Hadigheh, S.A., Mahini, S.S. and Maheri, M.R. (2014), "Seismic behavior of FRP-retrofitted reinforced concrete frames", *J. Earthq. Eng.*, **18**, 1171-1197.
- IS:1786-2008 (2008), High Strength Deformed Steel Bars and Wires for Concrete reinforcement — Specifications; Bureau of Indian Standards, New Delhi, India.
- IS 456 (2000), Code of practice for plain and reinforced concrete; (Fourth Revision), Bureau of Indian Standards, New Delhi, India.
- Kalogeropoulos, G.I., Tsonos, A.D.G., Konstantinidis, D. and Tsetines, S. (2016), "Pre-earthquake and post-earthquake retrofitting of poorly detailed exterior RC beam-to-column

- joints”, *Eng. Struct.*, **109**, 1-15.
- Kanchanadevi, A. and Ramanjaneyulu, K. (2017), “Comparative performance of seismically deficient exterior beam-column sub-assemblages of different design evolutions: A closer perspective”, *Earthq. Struct., Int. J.*, **13**(2), 177-191.
- Kheyroddin, A., Khalili, A., Emami, E. and Sharbatdar, M.K. (2016), “An innovative experimental method to upgrade performance of external weak RC joints using fused steel prop plus sheets”, *Steel Compos. Struct., Int. J.*, **21**(2), 443-460.
- Pampanin, S. and Christopoulos, C. (2003), “Non-invasive Retrofit of Existing RC Frames Designed for Gravity Loads Only”, *Proceedings of the Fib Symposium on Concrete Structures in Seismic Regions*, Greece.
- Pampanin, S., Christopoulos, C. and Chen, T.H. (2006), “Development and validation of a metallic haunch seismic retrofit solution for existing under-designed RC frame buildings”, *Earthq. Eng. Struct. Dyn.*, **35**, 1739-1766.
- Pampanin, S., Bolognini, D. and Pavese, A. (2007), “Performance-Based Seismic Retrofit Strategy for Existing Reinforced Concrete Frame System Using Fiber-Reinforced Polymer Composites”, *J. Compos. Constr. ASCE*, **11**, 211-226.
- Paulay, T. and Priestley, M.N.J. (1992), “Seismic design of reinforced concrete and masonry building”, Wiley Interscience publication.
- Prota, A., Nanni, A., Manfredi, G. and Cosenza, E. (2004), “Selective Upgrade of Under designed Reinforced Concrete Beam-Column Joints Using Carbon Fiber-Reinforced Polymers”, *ACI Struct. J.*, **101**(5), 699-707.
- Realfonzo, R., Napoli, A. and Pinilla, J.G.R (2014), “Cyclic behavior of RC beam-column joints strengthened with FRP systems”, *Constr. Build. Mater.*, **54**, 282-297.
- Santarsiero, G. and Masi, A. (2015), “Seismic performance of RC beam-column joints retrofitted with steel dissipation jackets”, *Eng. Struct.*, **85**, 95-106.
- Sezen, H. (2012), “Repair and Strengthening of Reinforced Concrete Beam-Column Joints with Fiber-Reinforced Polymer Composites”, *J. Compos. Constr.*, **16**(5), 499-506.
- Shafaei, J., Hosseini, A. and Marefat, M.S. (2014), “Seismic retrofit of external RC Beam-column joints by joint enlargement using prestressed steel angles”, *Eng. Struct.*, **81**, 265-288.
- Shannag, M.J., Barakat, S. and Abdul-Kareem, M. (2002), “Cyclic behaviour of HPFRC-repaired reinforced concrete interior beam-column joints”, *Mater. Struct./Materiaux et Constr.*, **35**, 348-356.
- Sharbatdar, M.K., Kheyroddin, A. and Emami, E. (2012), “Cyclic performance of retrofitted reinforced concrete beam-column joints using steel prop”, *Constr. Build. Mater.*, **36**, 287-294.
- Sharma, A. (2013), “Seismic Behavior and Retrofitting of RC Frame Structures with Emphasis on Beam-Column Joints – Experiments and Numerical Modeling”, Doctor of Philosophy Thesis; University of Stuttgart.
- Sharma, A., Reddy, G.R., Eligehausen, R., Genesio, G. and Pampanin, S. (2014), “Seismic Response of Reinforced Concrete Frames with Haunch Retrofit Solution”, *ACI Struct. J.*, **111**(3), 673-684.
- SP34 (1987), Handbook on concrete reinforcement and detailing; Bureau of Indian Standards, New Delhi, India.
- Tsonos, A.G. (1999), “Lateral Load Response of Strengthened Reinforced Concrete Beam-to-Column Joints”, *ACI Struct. J.*, **96**(1), 46-56.
- Tsonos, A.G. (2014), “A new method for earthquake strengthening of old R/C structures without the use of conventional reinforcement”, *Struct. Eng. Mech., Int. J.*, **52**(2), 391-403.
- Yilmaz, S., Özen, M.A. and Yardım, Y. (2013), “Tensile behavior of post-installed chemical anchors embedded to low strength concrete”, *Constr. Build. Mater.*, **47**, 861-866.
- Yu, Q.S., Uang, C.M. and Gross, J. (2000), “Seismic rehabilitation design of steel moment connection with welded haunch”, *J. Struct. Eng. ASCE*, **126**(1), 69-78.
- Yurdakul, O. and Avşar, O. (2015), “Structural repairing of damaged reinforced concrete beam-column assemblies with CFRPs”, *Struct. Eng. Mech., Int. J.*, **54**(3), 521-543.

CC